a major cause of secondary carnitine deficiency even in healthy children (Stanley 2004). Ten days before the onset of the Reye-like syndrome, she had a cold and was given Cefteram pivoxil (CFTM-PI) for four days. The initial serum acylcarnitine profile showed no elevation of hydroxy-C5 carnitine, nor of pivaloylcarnitine. While the antibiotic might have contributed to secondary carnitine deficiency in part, the acute attack with fasting was more likely the course of the low carnitine in the patient at presentation.

The time-course changes in the serum and urinary acylcarnitine levels after L-carnitine supplementation were studied. These changing profiles suggest that accumulated and potentially toxic long-chain acylcarnitines in the mitochondria were eliminated from the body by day 13. The majority of accumulated long-chain acylcarnitines in the mitochondria may be eliminated by the following steps: 1) a large amount of accumulated long-chain acylcarnitines should be transferred from the mitochondrial matrix by carnitine acylcarnitine translocase if there is a sufficient amount of free carnitine outside of the mitochondrial matrix; 2) then peroxisomal beta-oxidation reduces the chain length of such accumulated fatty acids; 3) the resultant medium-chain fatty acids can be catalyzed in the mitochondria, or further ω-oxidized into dicarboxylic acids in the microsomes; 4) these medium-chain DC and their carnitine conjugates can be excreted into the urine efficiently. It took several days for oral L-carnitine administration to increase the serum carnitine levels, probably because the intracellular stores were depleted and it took several days for them to be replenished. Thereafter, the administration increased the excretion of abnormal acylcarnitines, some of which had probably accumulated within the tissues.

It is noteworthy that the acetylcarnitine in both the serum and the urine was a predominant acylcarnitine on day 7 (Fig. 1). Elevation of acetylcarnitine in the serum and urine indicates the presence of enough acetyl-CoA in the mitochondria and the availability of acetyl-CoA for carnitine acyltransferase reactions in the cells, and might account for the increased beta-oxidation rates upon L-carnitine therapy (Fontaine et al. 1996). In general, acetylcarnitine is a major acylcarnitine in healthy controls and is regarded as a marker of undisturbed beta-oxidation (Costa et al. 1998). Since CPT2-deficient patients have beta-oxidation restrictions of long-chain acyl-CoA, L-carnitine supplementation may increase beta-oxidation of medium-chain acyl-CoAs, which could be supplied via peroxisomal beta-oxidation of long-chain acyl-CoA.

Carnitine supplementation in the treatment of long-chain beta-oxidation defects is still controversial. In patients with a defect in the mitochondrial beta-oxidation spiral, when a preceding L-carnitine deficiency is normalized, and transport into the mitochondria of long-chain fatty acids is also normalized, acyl-CoAs accumulate instead of being oxidized by the defective reaction and, consequently, in such cases, free CoA is depleted in the mitochondria (Yoshino et al. 2003). This may be true in beta-oxidation defects such as very long-chain acyl-CoA dehydrogenase (VLCAD) deficiency and trifunctional protein deficiency. Studies on VLCAD-deficient mice suggested carnitine supplementation results in the induction of acylcarnitine production in various tissues and significant accumulation of potentially toxic intermediate acylcarnitines in tissues (Liebig et al. 2006; Primassin et al. 2008). However, blockage of the CPT2 step causes the accumulation of long-chain acylcarnitines but does not primarily cause the accumulation of intermediate CoA esters in beta-oxidation.

Acknowledgment

This study was supported in part by Health and Labour Science Research Grants for Research on Children and Families from The Ministry of Health, Labour and Welfare of Japan.

References

Bonnefont, J.P., Demaugre, F., Prip-Buus, C., Saudubray, J.M., Brivet, M., Abadi, N. & Thuillier, L. (1999) Carnitine palmitoyltransferase deficiencies. *Mol. Genet. Metab.*, **68**, 424-440.

Bonnefont, J.P., Djouadi, F., Prip-Buus, C., Gobin, S., Munnich, A. & Bastin, J. (2004) Carnitine palmitoyltransferases 1 and 2: biochemical, molecular and medical aspects. *Mol. Aspects Med.*, **25**, 495-520.

Costa, C.G., Dorland, L., de Almeida, I.T., Jakobs, C., Duran, M. & Poll-The, B.T. (1998) The effect of fasting, long-chain triglyceride load and carnitine load on plasma long-chain acylcarnitine levels in mitochondrial very long-chain acyl-CoA dehydrogenase deficiency. *J. Inherit. Metab. Dis.*, **21**, 391-399.

Demaugre, F., Bonnefont, J.P., Colonna, M., Cepanec, C., Leroux, J.P. & Saudubray, J.M. (1991) Infantile form of carnitine palmitoyltransferase II deficiency with hepatomuscular symptoms and sudden death. Physiopathological approach to carnitine palmitoyltransferase II deficiencies. *J. Clin. Invest.*, **87**, 859-864.

Fontaine, M., Briand, G., Vallée, L., Ricart, G., Degand, P., Divry, P., Vianey-Saban, C. & Vamecq, J. (1996) Acylcarnitine removal in a patient with acyl-CoA beta-oxidation deficiency disorder: effect of L-carnitine therapy and starvation. *Clin. Chim. Acta*, **252**, 109-122.

Hug, G., Bove, K.E. & Soukup, S. (1991) Lethal neonatal multiorgan deficiency of carnitine palmitoyltransferase II. *N. Engl. J. Med.*, **325**, 1862-1864.

Kobayashi, H., Hasegawa, Y., Endo, M., Purevsuren, J. & Yamaguchi, S. (2007a) A retrospective ESI-MS/MS analysis of newborn blood spots from 18 symptomatic patients with organic acid and fatty acid oxidation disorders diagnosed either in infancy or in childhood. *J. Inherit. Metab. Dis.*, **30**, 606.

Kobayashi, H., Hasegawa, Y., Endo, M., Purevsuren, J. & Yamaguchi, S. (2007b) ESI-MS/MS study of acylcarnitine profiles in urine from patients with organic acidemias and fatty acid oxidation disorders. *J. Chromatogr. B Analyt. Technol. Biomed. Life Sci.*, **855**, 80-87.

Liebig, M., Gyenes, M., Brauers, G., Ruiter, J.P., Wendel, U., Mayatepek, E., Strauss, A.W., Wanders, R.J. & Spiekerkoetter, U. (2006) Carnitine supplementation induces long-chain acylcarnitine production—studies in the VLCAD-deficient mouse. *J. Inherit. Metab. Dis.*, **29**, 343-344.

Longo, N., Amat di San Filippo, C. & Pasquali, M. (2006) Disorders of carnitine transport and the carnitine cycle. *Am. J. Med. Genet. C. Semin. Med. Genet.*, **142C**, 77-85.

Mueller, P., Schulze, A., Schindler, I., Ethofer, T., Buehrdel, P. & Ceglarek, U. (2003) Validation of an ESI-MS/MS screening

method for acylcarnitine profiling in urine specimens of neonates, children, adolescents and adults. *Clin. Chim. Acta*, **327**, 47-57.

Primassin, S., Ter Veld, F., Mayatepek, E. & Spiekerkoetter, U. (2008) Carnitine supplementation induces acylcarnitine production in tissues of very long-chain acyl-CoA dehydrogenase-deficient mice, without replenishing low free carnitine. *Pediatr. Res.*, **63**, 632-637.

Stanley, C.A. (2004) Carnitine deficiency disorders in children. *Ann. N.Y. Acad. Sci.*, **1033**, 42-51.

Wataya, K., Akanuma, J., Cavadini, P., Aoki, Y., Kure, S., Invernizzi, F., Yoshida, I., Kira, J., Taroni, F., Matsubara, Y. & Narisawa, K. (1998) Two CPT2 mutations in three Japanese patients with carnitine palmitoyltransferase II deficiency: functional analysis and association with polymorphic haplotypes and two clinical phenotypes. *Hum. Mutat.*, **11**, 377-386.

Yoshino, M., Tokunaga, Y., Watanabe, Y., Yoshida, I., Sakaguchi, M., Hata, I., Shigematsu, Y., Kimura, M. & Yamaguchi, S. (2003) Effect of supplementation with L-carnitine at a small dose on acylcarnitine profiles in serum and urine and the renal handling of acylcarnitines in a patient with multiple âcyl-coenzyme A dehydrogenation defect. *J. Chromatogr. B Analyt. Technol. Biomed. Life Sci.*, **792**, 73-82.

Hepatology Research 2010; 40: 295–303 doi: 10.1111/j.1872-034X.2009.00594.x

Original Article

Histological findings in the livers of patients with neonatal intrahepatic cholestasis caused by citrin deficiency

Akihiko Kimura,[1] Masayoshi Kage,[2] Ikuo Nagata,[3] Sotaro Mushiake,[4] Toshihiro Ohura,[5] Yusaku Tazawa,[6] Shunichi Maisawa,[7] Takeshi Tomomasa,[8] Daiki Abukawa,[5] Yoshiyuki Okano,[9] Ryo Sumazaki,[10] Masaki Takayanagi,[11] Akiko Tamamori,[12] Tohru Yorifuji,[13] Yasuhiko Yamato,[1] Kohji Maeda,[1] Masami Matsushita,[1] Toyojiro Matsuishi,[1] Ken Tanikawa,[2] Keiko Kobayashi[14] and Takeyori Saheki[14]

[1]Department of Pediatrics and Child Health, [2]Department of Pathology, Kurume University School of Medicine, Kurume, [3]Department of Pediatrics, Faculty of Medicine, Tottori University, Yonago, [4]Department of Pediatrics, Faculty of Medicine, Osaka University, Osaka, [5]Department of Pediatrics, Tohoku University School of Medicine, Sendai, [6]Department of Pediatrics, South Miyagi Medical Center, Shibata, [7]Department of Pediatrics, Morioka Children's Hospital, Morioka, [8]Department of Pediatrics, Gunma University School of Medicine, Maebashi, [9]Department of Pediatrics, Osaka City University Graduate School of Medicine, Osaka, [10]Department of Pediatrics, Institute of Clinical Medicine, University of Tsukuba, Tsukuba, [11]Department of Pediatrics, Chiba Children's Hospital, Chiba, [12]Department of Pediatrics, Fujiidera City Hospital, Fujiidera, [13]Department of Pediatrics, Kyoto University, Kyoto, and [14]Department of Molecular Metabolism and Biochemical Genetics, Kagoshima University Graduate School of Medical and Dental Sciences, Kagoshima, Japan

Aim: To characterize the histological features of the livers of patients with neonatal intrahepatic cholestasis caused by citrin deficiency (NICCD), we studied specimens from 30 patients diagnosed with NICCD by genetically analyzing the *SLC25A13* gene.

Methods: Liver biopsy specimens were subjected to hematoxylin–eosin, Azan, and Berlin-blue staining.

Results: Most specimens showed varying degrees of fibrosis. The degree of inflammation varied among the specimens, with half showing moderate or severe inflammatory changes. Fat deposition in hepatocytes was observed in almost all of the specimens, and severe fatty liver was noted in 20 (67%) of them. There was a mixture of two types of hepatocytes with macrovesicular or microvesicular fat droplets, and cholestasis was observed at a rate of 77%. Hemosiderin deposition, mostly mild and localized in periportal hepatocytes and macrophages in portal areas, was observed in 57% of the specimens.

Conclusion: A combination of mixed macrovesicular and microvesicular fatty hepatocytes and the above-described findings, such as fatty liver, cholestasis, necroinflammatory reaction and iron deposition, are almost never observed in other liver diseases in infants and adults. We believe that NICCD is a disease with characteristic hepatopathological features.

Key words: citrin, citrullinemia, fatty liver, fibrosis, neonatal intrahepatic cholestasis caused by citrin deficiency, *SLC25A13*.

INTRODUCTION

SAHEKI *ET AL.* reported that the enzyme abnormalities of citrullinemia can be classified as qualitative, type I and type III, or quantitative, type II.[1,2] The first, the classical form (CTLN1), is found in most patients with neonatal/infantile-onset citrullinemia, and was first described by McMurray *et al.*[3] In CTLN1, the enzyme defect is found in all tissues in which argininosuccinate synthetase (ASS) is expressed.[1,2,4] The second form, type II citrullinemia (CTLN2) is an adult- or late childhood-onset liver disease characterized by a liver-specific defect in ASS, and most of these patients have a fatty liver.[5] This enzyme abnormality is caused by a deficiency in citrin, a calcium-binding

Correspondence: Professor Masayoshi Kage, Department of Pathology, Kurume University School of Medicine, 67 Asahi-machi, Kurume 830-0011, Japan. Email: masakage@med.kurume-u.ac.jp
Received 27 February 2008; revision 22 July 2009; accepted 9 August 2009.

mitochondrial solute carrier protein which is encoded by the *SLC25A13* gene.[6]

Recently, several cases of *SLC25A13* mutations have been reported in early infancy with cholestatic liver disease.[7–13] Yamaguchi *et al.*[14] designated these findings as neonatal intrahepatic cholestasis caused by citrin deficiency (NICCD). Citrin deficiency causes two age-dependent phenotypes, CTLN2 in adults and NICCD in infants.[15] Most NICCD patients showed hypoproteinemia, galactosemia, multiple aminoacidemia including citrullinemia, methionemia and tyrosinemia, cholestasis, and have a fatty liver.[7–13] Only a few papers have described the pathology of the NICCD[8,9,11,13] or CTLN2[5] liver.

Therefore, the present study was designed to clarify the histological findings of the NICCD liver.

METHODS

Patients

WE STUDIED THE liver histological findings of 30 patients aged 2.9 ± 1.7 months with a range of 1–7 months consisting of 17 men and 13 women who had been diagnosed with NICCD with *SLC25A13* mutations by genetic analysis including five patients who were documented in previous reports.[7–11] Moreover, mutations in *SLC25A13* were detected in both alleles of 29 patients and in a single allele of one patient. Mutation detection and DNA diagnosis of the *SLC25A13* gene were performed as previously described ([6,14,16] and T. Saheki et al., 2006, unpublished data). Moreover, we examined biochemical data within 1 week before or after liver biopsy for 30 patients with NICCD.

Methods

Liver biopsy specimens from 30 patients diagnosed with NICCD were subjected to hematoxylin–eosin, Azan, and Berlin-blue staining. The grading of fibrosis and inflammation was based on Ludwig's Classification with slight modifications (Table 1).[17] The other histopathological features were graded as none, mild, moderate and severe, and scored as 0, 1, 2 and 3, respectively.

Grading was independently performed by three pathologists, and the grade for each specimen was determined by consensus between two or three of them.

Relationship between age and histological findings

To clarify the relationship between age and the histological findings, the cases were divided into three groups according to their ages: group A, less than 2 months old; group B, 3–4 months old; and group C, more than 5 months old. The average of the grading score of the histological findings for each group was then obtained.

Table 1 Histological classification of liver biopsy

Stage of fibrosis	
Stage 0	No portal fibrosis
Stage 1	Mild to moderate fibrous expansion of portal tract
Stage 2	Bridging fibrosis between portal tracts without lobular distortion
Stage 3	Bridging fibrosis between portal tracts with lobular distortion
Stage 4	Liver cirrhosis
Grade of inflammation	
Grade 0	None (0)
Grade 1	Mild (1–3)
Grade 2	Moderate (4–6)
Grade 3	Severe (≥7)

Parentheses indicate scores derived by Ludwig's scoring system.

Statistical analysis

The data regarding the relationship between age and histological findings were analyzed using the Mantel–Haenszel linear trend test. *P*-values less than 0.05 were regarded as statistically significant.

RESULTS

Patients

THE PROGNOSIS OF almost NICCD patients at 1 year of age was fairly well. However, some NICCD patients had developed progressive liver failure by then. For example, two patients developed liver failure by 6 months (patient 28) and 7 months (patient 30)[10] of age and one patient (patient 9) developed behavioral aberrations, which included shouting and episodes of violence, by 16 years of age.[9,18] Two patients, one with liver failure[10] and one with mental derangement,[9,18] received a living-related liver transplant. Therefore, the outcomes of the NICCD patients were not always favorable. We obtained four sets of follow-up liver biopsy specimens from patients 8, 9, 13 and 18 (data not shown).

From the clinical laboratory data, serum levels of citrulline, α-fetoprotein, ferritin and pancreatic secretory trypsin inhibitor (PSTI) were noted to have generally increased (Table 2). We also detected high serum levels of total and direct bilirubin, aspartate (AST) and/or alanine aminotransferase (ALT), total bile acids and

Table 2 Biochemical data on liver biopsy in the 30 patients with neonatal intrahepatic cholestasis caused by citrin deficiency

Patient No.	1	2	3	4	5	6	7	8	9	10	11
Age (months)/sex	1/M	1/M	1/M	1/M	1/F	1/F	2/M	2/M	2/M	2/M	2/M
Total/direct bilirubin (mg/dL)	9.0/3.4	12.6/2.6	3.3/2.2	10.4/5.8	5.6/1.9	3.3/0.7	6.2/3.8	9.9/5.4	7.6/3.3	6.6/2.6	3.6/1.6
AST/ALT (IU/L)	96/38	31/20	115/61	121/24	62/41	43/21	112/28	109/50	41/20	100/30	190/53
Total bile acids (μM)	250	120	513	298	210	52	323	331	n.d.	240	212
γ-GTP (IU/L)	206	142	131	251	186	148	142	408	130	n.d.	125
Total cholesterol (mg/dL)	212	195	n.d.	181	161	158	175	206	133	n.d.	196
Total protein/albumin (g/dL)	4.9/3.2	3.9/2.6	5.3/4.0	4.5/3.0	5.1/3.5	4.4/3.3	4.7/2.6	-/-	3.6/1.9	-/-	4.7/2.8
Citrulline (nmol/mL)	4.3	n.d.	85.0	n.d.	40.5	149.0	74.3	12.6	n.d.	117.0	211.0
α-Fetoprotein (ng/mL)	n.d.	n.d.	n.d.	200 700	n.d.	n.d.	n.d.	n.d.	29 600	n.d.	n.d.
PSTI (ng/mL)	n.d.	n.d.	n.d.	91.0	n.d.	40.0	24.0	n.d.	n.d.	n.d.	110.0
Ferritin (ng/mL)	447	n.d.	n.d.	2656	n.d.	117	502	1830	n.d.	n.d.	n.d.
Prothrombin activity (%)	75	26	93	55	37	88	70	37	9	n.d.	76
Mutation type	V/XIX	I/II	I/I	I/II	II/II	I/V	II/V	II/V	II/II	I/V	I/V

12	13	14	15	16	17	18	19	20	21	22	23	24	25	26
2/M	2/F	2/F	2/F	2/F	3/M	3/M	3/M	3/F	3/F	4/M	4/M	4/F	4/F	5/M
10.2/3.9	11.1/3.6	13.0/8.5	6.9/2.7	5.3/2.4	6.1/3.5	6.0/3.8	9.6/2.7	8.8/3.2	12.0/2.6	5.1/2.5	6.7/3.7	5.4/3.5	6.2/2.4	15.0/10.1
106/22	86/23	133/45	78/25	74/44	98/36	232/48	85/44	95/39	75/19	95/90	295/105	208/100	83/24	146/66
240	320	172	290	143	302	269	205	389	157	283	172	253	127	355
213	132	78	209	160	124	249	n.d.	149	198	145	270	132	90	129
n.d.	n.d.	204	232	n.d.	194	n.d.	140	223	256	128	169	n.d.	n.d.	n.d.
4.9/3.7	4.0/3.5	3.8/2.6	4.1/2.7	n.d.	5.3/3.9	n.d.	5.7/3.8	5.1/3.1	4.8/3.0	4.2/3.5	4.8/3.1	5.5/3.5	n.d.	4.0/2.8
242.0	478.0	581.0	n.d.	291.7	839.1	208.0	n.d.	32.2	392.0	675.0	524.0	27.5	28.4	5.8
n.d.	n.d.	87 000	n.d.	91 940	n.d.	n.d.	n.d.	n.d.	n.d.	75 300	n.d.	n.d.	n.d.	10 578
n.d.	24.0	n.d.	n.d.	57.0	n.d.	n.d.	n.d.	62.0	12.9	12.5	n.d.	n.d.	n.d.	188.0
743	n.d.	775	n.d.	1651	n.d.	n.d.	n.d.	n.d.	200	n.d.	n.d.	503	n.d.	n.d.
87	n.d.	n.d.	25	51	43	n.d.	66	50	75	29	39	69	15	15
IV/IV	II/II	II/V	II/II	II/II	II/III	I/I	II/II	VI/VI	I/II	I/–	I/II	VIII/X	IV/VI	II/V

27	28	29	30	Mean ± SD	Range	Normal range
5/F	6/M	6/F	7/F			
5.8/3.4	5.5/3.9	6.2/2.0	5.9/2.9	7.6 ± 3.0/3.6 ± 2.0 (n = 30)	3.3–15.0/0.7–10.1	0.2–1.1/0.0–0.4
260/169	123/87	127/38	191/67	120.3 ± 63.7/49.2 ± 33.3 (n = 30)	31–295/20–169	6–40/5–40
213	n.d.	150	168	241.3 ± 96.1 (n = 28)	52–513	5–25
67	149	65	292	168.6 ± 75.0 (n = 28)	65–408	5–32
n.d.	148	n.d.	168	183.1 ± 34.8 (n = 19)	133–256	130–220
6.4/4.7	4.5/3.0	4.6/2.7	6.0/3.2	4.7 ± 0.7/3.2 ± 0.6 (n = 25)	3.6–6.4/1.9–4.7	6.5–8.3/3.7–5.2
48.2	11.0	41.3	86.8	179.1 ± 199.2 (n = 25)	4.3–291.7	17–43
n.d.	11 000	329 000	207 000	115 790.9 ± 108 111.0 (n = 9)	11 000–329 000	<10 000
n.d.	n.d.	21.9	n.d.	58.5 ± 53.6 (n = 11)	12.5–188.0	22–46
n.d.	n.d.	n.d.	197	874.6 ± 816.3 (n = 11)	117–2656	12–80
88	9	41	29	51.3 ± 26.0 (n = 25)	9–93	70–140
I/II	I/II	I/II	I/II			

AST, aspartate aminotransferase; ALT, alanine aminotransferase; γ-GTP, γ-glutamyl transpeptidase; PSTI, pancreatic secretory trypsin inhibiter; M, male, F, female; n.d., not done; I, 851del4; II, IVS11 + 1G > A; III, 1638ins23; IV, S225X; V, IVS13 + 1G > A; VI, 1800ins1; VIII, E601X; X, IVS6 + 5G > A; XIXIVS16ins3kb; –, unknown; SD, standard deviation.

γ-glutamyl transpeptidase. Prothrombin activity, total protein and albumin were decreased. The mutation types were 851del4/IVS11 + 1G > A throughout most of late infancy, being more than 5 months of age in patients 27, 28, 29 and 30.

Histological findings

Histological findings of the 30 patients are shown in Table 3. The results of the fibrosis staging and inflammation grading are shown in Figure 1.

Fibrosis

Most specimens showed varying degrees of fibrosis; 35% of all specimens were classified as stage 0, while stages 1 and 2 together accounted for 50%. However, there was a wide spectrum of fibrosis: more advanced liver lesions with distorted lobular architecture (stage 3) (Fig. 2) and cirrhosis were observed in four and one specimens, respectively. One patient with cirrhosis developed hepatic failure. Therefore, this patient underwent a living-related liver transplant. One patient with cirrhosis developed at 10 months of age.[10]

Inflammatory reaction

The degree of inflammation varied with the specimens, where half showed moderate or severe inflammatory changes. Inflammatory cell infiltration in the portal tracts and piecemeal necrosis were observed (Fig. 3). Inflammatory cells present in the portal tracts were predominantly lymphocytes. Focal necrosis and acidophilic bodies in the parenchyma were seen in 23 (77%) and 12 (40%) specimens, respectively. The sinusoids showed the proliferation of mononuclear cells with scarce neutrophils and the activation of Kupffer cells.

Fat deposition in hepatocytes

Fat deposition in hepatocytes was observed in all specimens except one and severe fatty liver was noted for 20 (67%) specimens (Fig. 4a). Fat droplets deposited in the cytoplasm of hepatocytes varied in size, and fat-laden hepatocytes were classified as those with macrovesicular fat droplets, those with foamy, microvesicular fat droplets, and those with mixed macrovesicular and microvesicular fat droplets. Hepatocytes with microvesicular fat droplets had a centrally located nucleus. In 80% of 29 specimens with fat deposition including all 20 specimens which showed severe fatty livers, there was a mixture of macro- and microvesicular fat droplets (Fig. 4b,c). Macrovesicular and microvesicular fatty liver alone accounted for three (10%) and one (4%) specimens, respectively. A moderate and severe fatty liver with an inflammatory reaction and lipogranuloma were diagnosed as steatohepatitis, which accounted for 60% of the patients. The histopathological findings in this disease were different from those in non-alcoholic steatohepatitis. The clinical features of one patient who had no fat deposition in hepatocytes did not differ from that of other patients with such fat deposition.

Cholestasis

Cholestasis was observed in 77% of the specimens and was severe in 57%. The acinar arrangement of hepatocytes was prominent in specimens with severe cholestasis (Fig. 5) and multinucleated giant cell transformation was found in one case (Fig. 6).

Hemosiderin deposition

Hemosiderin deposition, mostly mild and localized in periportal hepatocytes and macrophages in portal areas (Fig. 4b), was observed in 57% of the specimens.

A combination of all five features, fatty liver, inflammatory cell infiltration, fibrosis, cholestasis and hemosiderin deposition was observed in the same liver biopsy specimen in 12 (40%) of the total specimens.

Relationship between the age and the histological findings

The mean score of each histological finding in each of groups A, B and C are summarized in Table 4. The degree of fibrosis, necroinflammatory reaction such as focal necrosis and acidophilic bodies, acinar arrangement of hepatocytes, cholestasis and steatohepatitis of infants more than 3 months old (groups B and C) were more accentuated than those of the early infants of group A. Conversely, hemosiderosis and extramedullary hematopoiesis in groups B and C were less pronounced than in group A. The staging score of fibrosis, grade of inflammation and steatohepatitis were significantly higher in the older than in the younger group in order of group A, B and C.

Histological findings of follow-up biopsy

Follow-up biopsies were conducted for patients 8, 9, 13 and 18, and the findings were as follows: patients 8, 9 and 13 showed histological deterioration of cholestasis and fatty change. Of note, patient 9 underwent a liver transplant at the age of 16 years because of hepatic failure. The findings for the explant liver were

Table 3 Histological findings of liver biopsy in the 30 patients with neonatal intrahepatic cholestasis caused by citrin deficiency

Patient no.	1	2	3	4	5	6	7	8	9	10
Stage of fibrosis	0	0	1	0	0	0	0	0	3	2
Grade of inflammation	1	2	2	1	1	1	2	1	1	1
Focal necrosis[a]	1	1	2	0	0	0	1	0	0	1
Acidophilic body[b]	0	1	0	2	0	1	0	1	0	0
Acinar arrangement[c]	0	1	3	3	0	1	0	1	2	1
Cholestasis[d]	0	3	3	3	1	0	1	2	3	1
Degree of fat deposit[e]	1	3	3	3	3	3	2	3	3	3
Type of fat deposit[f]	1	3	0	3	3	3	1	3	0	0
Steatohepatitis[g]	0	1	1	1	0	1	1	1	0	2
Hemosiderosis[h]	0	2	1	2	0	0	1	2	0	2
Extramedullary hematopoiesis[i]	0	2	0	3	2	1	0	2	0	0
Patient no.	11	12	13	14	15	16	17	18	19	20
Stage of fibrosis	0	2	2	1	0	0	3	2	1	1
Grade of inflammation	1	1	1	2	1	2	2	2	3	1
Focal necrosis	1	0	1	1	1	2	1	1	3	0
Acidophilic body	1	0	0	1	0	0	1	0	0	0
Acinar arrangement	2	0	0	2	2	1	1	1	2	1
Cholestasis	3	0	0	3	3	2	2	2	3	3
Degree of fat deposit	3	0	2	2	3	2	3	3	2	3
Type of fat deposit	3	0	2	3	3	3	3	3	3	3
Steatohepatitis	2	0	0	1	1	1	1	1	2	1
Hemosiderosis	2	0	1	0	2	1	1	0	2	1
Extramedullary hematopoiesis	0	0	0	3	2	0	1	0	0	0
Patient no.	21	22	23	24	25	26	27	28	29	30
Stage of fibrosis	2	2	0	2	2	3	1	3	3	4
Grade of inflammation	3	2	1	2	3	2	1	2	3	3
Focal necrosis	1	2	1	1	3	1	1	1	2	1
Acidophilic body	1	2	0	1	1	1	0	0	0	2
Acinar arrangement	3	2	0	2	2	1	2	1	3	2
Cholestasis	3	3	0	3	0	3	3	3	3	3
Degree of fat deposit	3	3	3	3	1	3	2	3	3	3
Type of fat deposit	3	3	3	3	1	3	3	3	3	3
Steatohepatitis	0	3	2	1	0	2	1	3	3	3
Hemosiderosis	3	1	1	1	0	1	1	0	0	0
Extramedullary hematopoiesis	1	0	1	1	2	0	0	0	1	0

[a]Focal necrosis was graded from 0–3 based on the number of counts per 10 fields at a magnification of ×40. A score of denotes 0 is none, 1 denotes 1–2; 2 denotes up to 4, and 3 denotes >4.
[b]Acidophilic bodies were counted and graded from 0–3, as similar to that for focal necrosis.
[c]The acinar arrangements of the hepatocytes were graded 0–3. A rating of 0 denotes none, 1 denotes involvement up to 30% of the hepatocytes, 2 denotes 30–60%, and 3 denotes >60%.
[d]Cholestasis was graded from 0–3. A score of 0 denotes none, 1 denotes cholestasis without a bile plug, 2 denotes scattered bile plugs, and 3 denotes frequent bile plugs.
[e]The degree of fat deposition in hepatocytes was graded from 0–3 based on the percentage of hepatocytes in the biopsy involved. A rating of 0 denotes none; 1 denotes up to 30%, 2 denotes 30–60%, and 3 denote >60%.
[f]The type of fat deposit was classified as being between 0–3. A score of 0 denotes no fatty change, 1 denotes predominantly macrovesicular fat droplets, 2 denotes predominantly microvesicular fat droplets, and 3 denotes mixed microvesicular and macrovesicular fat droplets.
[g]Steatohepatitis was graded from 0–3, where 0 denotes none, 1 denotes steatosis involving up to 60% and intra-acinar inflammation with no or mild portal inflammation, 2 denotes steatosis (>66%) with both acinar and portal inflammation, and 3 denotes panacinar steatosis with intra-acinar inflammation and piecemeal necrosis.
[h]Hepatocellular iron was graded between 0–3, where 0 denotes none, 1 denotes localized deposition in the portal and /or periportal area; 2 denotes iron deposition involving up to 60% of the parenchyma, and 3 denotes >60%.
[i]Extramedullary hematopoiesis was graded between 0–3, similar to that for focal necrosis.

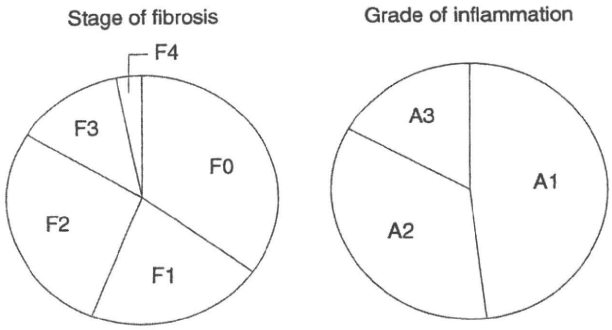

Figure 1 Results of fibrosis and the grade of necroinflammation.

more pronounced than those of the biopsy. Patient 8 showed progression of fibrosis from stage 1–3 and more pronounced portal inflammation. In contrast, patient 18 showed marked improvement of every

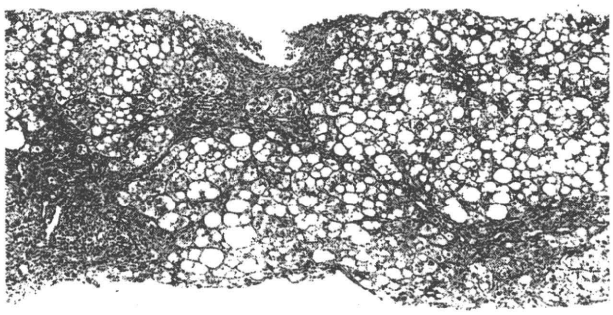

Figure 2 Severe fatty liver with distorted lobular architecture due to extensive fibrosis in stage 3 with portal inflammation (hematoxylin–eosin, original magnification ×50).

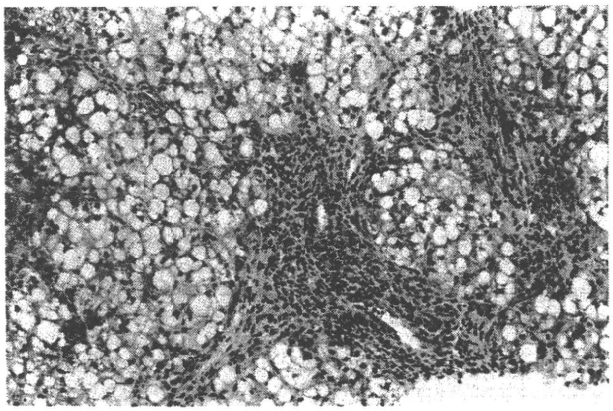

Figure 3 Fatty liver with moderate inflammatory cell infiltration in the portal tract and parenchyma, which is indicative of steatohepatitis (hematoxylin–eosin, original magnification ×100).

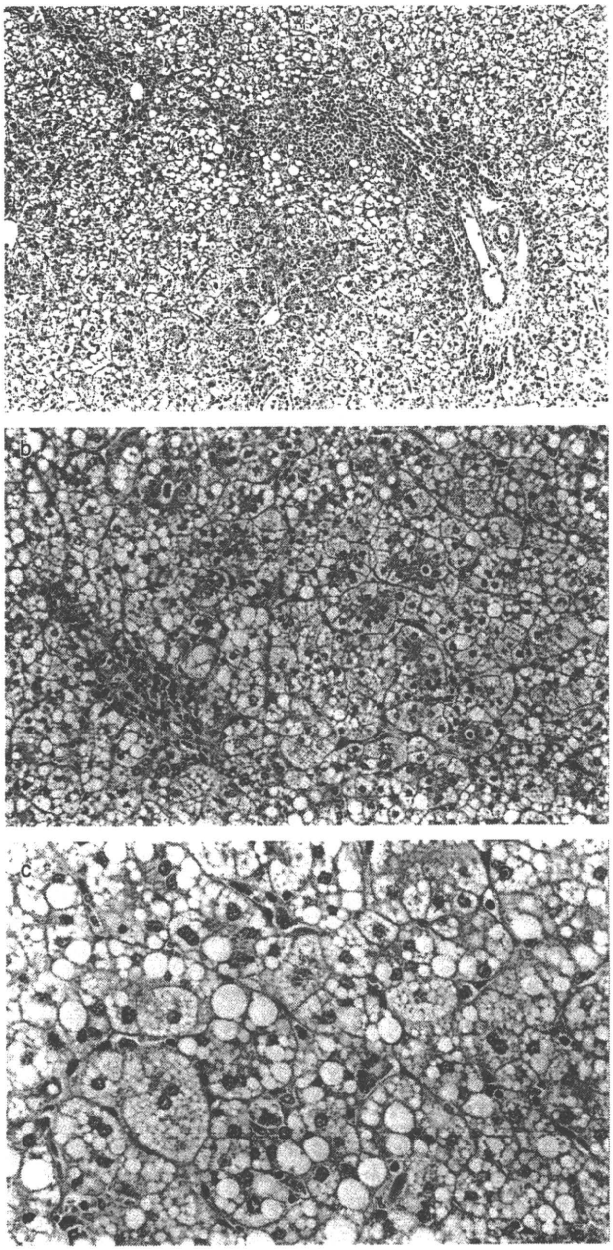

Figure 4 (a) Severe fatty liver with cholestasis. The portal tracts show mild inflammatory cell infiltration (hematoxylin–eosin [HE], original magnification ×50). (b) Pseudo-acinor transformation with bile plugs is observed. Hemosiderin-laden macrophages are present in a portal tract (HE, original magnification ×100). (c) Macro- and microvesicular-type fatty droplets. Some of the swollen hepatocytes have a foamy appearance and their cytoplasm packed with micro-fat droplets. Kupffer cells are activated (HE, original magnification ×200).

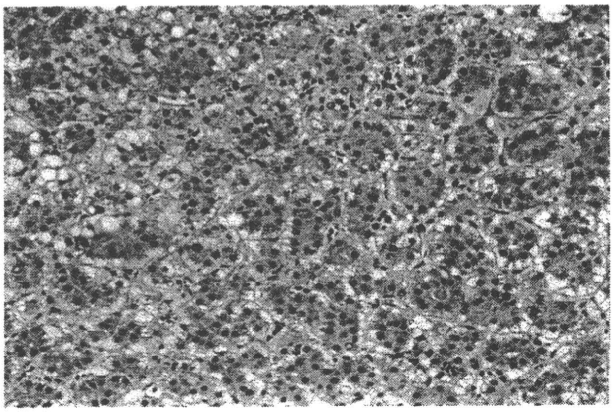

Figure 5 Striking pseudo-acinor transformation of the hepatic cords containing bile plugs. Small fatty droplets are present at the periphery of hepatocytes arranged in an acinar fashion (hematoxylin–eosin, original magnification ×100).

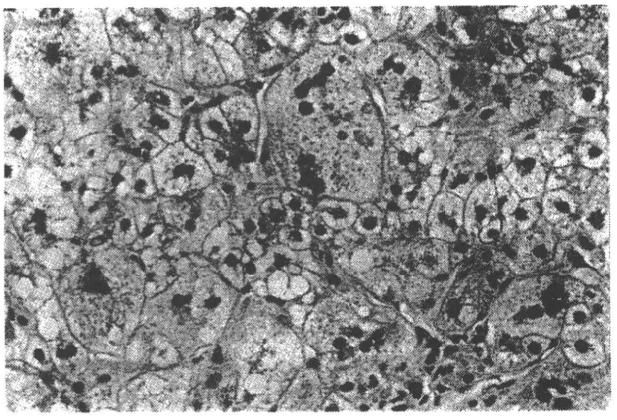

Figure 6 Giant cell hepatitis and cholestasis. Multinucleate giant cells contain several nuclei (hematoxylin–eosin, original magnification ×200).

histological finding, including decreased portal fibrosis and inflammation.

DISCUSSION

THE CAUSE OF liver dysfunctions such as fatty liver, hypoglycemia and galactosemia in this disease is as follows.[15] Citrin deficiency blocks the malate aspartate shuttle, which may increase the ratio of cytosolic nicotinamide adenine dinucleotide (NADH) to oxidized nicotinamide adenine dinucleotide ($NADH/NAD^+$), which in turn is associated with the inhibition of glycolysis and makes reduced alcohol metabolism. This may be why CTLN2 patients dislike carbohydrates and cannot drink alcohol, and why alcohol consumption often results in psychiatric symptoms. An increased $NADH/NAD^+$ ratio is also characteristic of the inhibition of gluconeogenesis involving reduced substrates.[19] This, together with the reduction in alanine metabolization to urea and glucose due to citrin deficiency may cause hypoglycemia in NICCD patients. Although NICCD patients suffer from galactosemia, which sometimes even leads to the development of cataracts, no abnormalities in the enzymes involved in galactose metabolism have been found.[20] Because uridine diphosphate-glucose epimerase which requires NAD as a cofactor is strongly inhibited by NADH,[21] galactosemia in NICCD may represent a high NADH level in the cytosol of the liver.

From the biochemical data of this study, 50% of the high level of total bilirubin was associated with direct bilirubin, but it was not always dominant. The levels of AST were increased to more than twice the levels of ALT. Low levels of total protein, albumin and prothrombin

Table 4 Relationship between age and histological changes

Pathological findings	Group A ($n = 16$) <2 months	Group B ($n = 9$) 3–4 months	Group C ($n = 5$) >5 months	*P*-value
Stage of fibrosis	0.69 ± 1.01	1.67 ± 0.87	2.80 ± 1.10	$P = 0.001$
Grade of inflammation	1.31 ± 0.48	2.11 ± 0.78	2.20 ± 0.84	$P = 0.004$
Focal necrosis	0.75 ± 0.68	1.44 ± 1.01	1.20 ± 0.45	$P = 0.063$
Acidophilic body	0.44 ± 0.63	0.67 ± 0.71	0.60 ± 0.89	$P = 0.523$
Acinar arrangement	1.19 ± 1.05	1.56 ± 0.88	1.80 ± 0.84	$P = 0.172$
Cholestasis	1.75 ± 1.29	2.11 ± 1.27	3.00 ± 0.00	$P = 0.059$
Degree of fat deposit	2.44 ± 0.89	2.67 ± 0.71	2.80 ± 0.45	$P = 0.333$
Steatohepatitis	0.81 ± 0.66	1.22 ± 0.97	2.40 ± 0.89	$P = 0.008$
Hemosiderosis	1.00 ± 0.89	1.11 ± 0.93	0.40 ± 0.55	$P = 0.356$
Extramedullary hematopoiesis	0.94 ± 1.18	0.67 ± 0.71	0.20 ± 0.45	$P = 0.297$

The data are expressed as means ± standard deviation.
P-values are by the Mantel–Haenszel linear trend test.

activity and high levels of citrulline, α-fetoprotein, ferritin and PSTI were observed as previously described in NICCD patients.[6–13] However, 11 patients showed high levels of ferritin, which were not observed in previous reports on NICCD patients. Therefore, the pediatric hepatologist should suspect NICCD when a neonatal cholestatic patient has high levels of AST of more than twice the ALT value, citrulline, α-fetoprotein and ferritin, and low levels of total protein and prothrombin activity.

The histological findings in this study such as a fatty liver, cholestasis, necroinflammatory reaction and iron deposition are not pathognomonic findings because they occur in various liver diseases.[22] However, the combination of mixed macrovesicular and microvesicular fatty hepatocytes and these histological findings are almost never observed in other liver diseases in infants and adults. Microvesicular fatty deposition was found in NICCD, this type of fatty change is a characteristic feature of Reye syndrome[23] and other rare conditions.[22] However, the histogenesis of the microvesicular fatty deposition in NICCD is unclear. It might reflect the acute impairment of β-oxidation of fatty acid due to mitochondrial dysfunction as in Reye syndrome.

Although our series of NICCD patients shared common liver histological findings as described above, there seemed a tendency that late infants of group C had more advanced fibrosis and more accentuated inflammation than those of early infants of group A. The duration of illness may be an aggravating factor of the progression of the disease in some cases. There was no difference between the liver histological findings and mutation type. Interestingly, however, the mutation type of patients with severe fibrosis who were 6 and 7 months of age was 851del4/IVS11 + 1G > A. Because evidence for this relationship between the mutation type and the progression of fibrosis is not clear, further investigation is needed. Moreover, in the follow-up liver biopsy patients, we observed improvements in their liver histological findings as the liver dysfunction was ameliorated. Therefore, we speculate that the correlations between the stage of the liver histological findings and the biochemical test data exist.

This study found that NICCD is a disease with characteristic hepatopathological features. If NICCD is suspected in the presence of cholestasis during infancy, a liver biopsy should be performed to screen for liver diseases. We believe that a liver biopsy is of high diagnostic value for NICCD, and is useful for accurately assessing inflammation and the degree of the progression of fibrosis.

Although we were not able to elucidate the natural history of the disease, we previously found that despite a benign course in the majority of the patients, it leads to the development of liver cirrhosis in some patients with CTLN2.[5,10] This suggests that it involves the risk of progressive fibrosis and eventually leads to the development of cirrhosis. This possibility is suggested by the above histopathological findings characteristic of NICCD in the patients who progressed to stage 3 chronic hepatitis and cirrhosis. Although the process responsible for the progression of liver lesions is not clear, some patients with steatohepatitis including non-alcoholic steatohepatitis (NASH) progress to cirrhosis.[24] In this study, steatohepatitis was found in 60% of the specimens. It is likely that, in NICCD, steatohepatitis repeatedly deteriorates, persists and progresses.

In conclusion, if NICCD is suspected in the presence of cholestasis during infancy, a liver biopsy should be performed to screen for other liver diseases. NICCD is a disease with characteristic hepatopathological features, such as the combination of mixed macrovesicular and microvesicular fatty hepatocytes, cholestasis, necroinflammatory reaction and iron deposition. Therefore, it is possible to diagnose NICCD based on histological liver findings in most cases. However, when cirrhosis with fat deposition is detected in hepatocytes in liver specimens, the patient should be carefully observed, because the prognosis of NICCD patients is not always fair, with some developing progressive liver failure by 1 year of age. Finally, we could not infer the development of CTLN2 from the histological findings of the patients with NICCD who were examined in this study.

ACKNOWLEDGMENTS

WE THANK DR S. Hattori (Biostatistics Center, Kurume University) for the excellent assistance in the statistical analyses.

REFERENCES

1 Saheki T, Tsuda M, Takada S *et al.* Role of argininosuccinate synthetase in the regulation of urea synthesis in the rat and argininosuccinate synthetase-associated metabolic disorder in men. *Adv Enzyme Regul* 1980; 18: 221–38.
2 Saheki T, Ueda A, Hosoya M *et al.* Qualitative and quantitative abnormalities of argininosuccinate synthetase in citrullinemia. *Clin Chim Acta* 1981; 109: 325–35.
3 McMurray WC, Mohyuddin F, Rossiter RJ *et al.* Citrullinuria: a new aminoaciduria associated with mental retardation. *Lancet* 1962; i: 138.

4 Saheki T, Kobayashi K, Ichiko H *et al.* Molecular basis of enzyme abnormalities in urea cycle disordwes: with special reference to citrullinemia and argininosuccinic aciduria. *Enzyme* 1987; **38**: 227–32.
5 Yagi Y, Saeki T, Imamura Y *et al.* The heterogenous distribution of argininosuccinate synthetase in the liver of type II citrullinemic patients: its specificity and possible clinical implications. *Am J Clin Pathol* 1988; **89**: 735–41.
6 Kobayashi K, Sinasac DS, Iijima M *et al.* The gene mutated in adult-onset type II citrullinemia encodes a putative mitochondrial carrier protein. *Nat Genet* 1999; **22**: 159–63.
7 Ohura T, Kobayashi K, Tazawa Y *et al.* Neonatal presentation of adult-onset type II citrullinemia. *Hum Genet* 2001; **108**: 87–90.
8 Tazawa Y, Kobayashi K, Ohura T *et al.* Infantile cholestatic jaundice associated with adult-onset type II citrullinemia. *J Pediatr* 2001; **138**: 735–40.
9 Tomomasa T, Kobayashi K, Kaneko H *et al.* Possible clinical and histologic manifestations of adult-onset type II citrullinemia in early infancy. *J Pediatr* 2001; **138**: 741–3.
10 Tamamori A, Okano Y, Ozaki H *et al.* Neonatal interahepatic cholestasis caused by citrin deficiency: severe hepatic dysfunction in an infant requiring liver transplantation. *Eur J Pediatr* 2002; **161**: 609–13.
11 Ohura T, Kobayashi K, Abukawa D *et al.* A novel inborn error of metabolism defected by elevated methionine and/or galactose in newborn screening: neonatal intrahepatic cholestasis caused by citrin deficiency. *Eur J Pediatr* 2003; **162**: 317–22.
12 Tamamori A, Fujimoto A, Okano Y *et al.* Effect of citrin deficiency in the perinatal period: feasibility of newborn mass screening for citrin deficiency. *Pediatr Res* 2004; **56**: 608–14.
13 Tazawa Y, Kobayashi K, Abukawa D *et al.* Clinical heterogeneity of neonatal intrahepatic cholestasis caused by citrin deficiency: case reports from 16 patients. *Mol Genet Metab* 2004; **84**: 213–9.
14 Yamaguchi N, Kobayashi K, Yasuda T *et al.* Screening of SLC25A13 mutations in early and late onset patients with citrin deficiency and in the Japanese population: identification of two novel mutations and establishment of multiple DNA diagnosis methods for nine mutations. *Hum Mutat* 2002; **19**: 122–30.
15 Saheki T, Kobayashi K. Mitochondrial aspartate glutamate carrier (citrin) deficiency as the cause of adult-onset type II citrullinemia (CTLN2) and idiopathic neonatal hepatitis (NICCD). *J Hum Genet* 2002; **47**: 333–41.
16 Yasuda T, Yamaguchi N, Kobayashi K *et al.* Identification of two novel mutations in the *SLC25A13* gene and detection of seven mutation in 102 patients with adult-onset type II citrullinemia. *Hum Genet* 2000; **107**: 537–45.
17 Ludwig J. The nomenclature of chronic active hepatitis: an obituary. *Gastroenterology* 1993; **105**: 274–8.
18 Kasahara M, Ohwada S, Takeichi T *et al.* Living-related liver transplantation for type II citrullinemia using a graft from heterozygote donor. *Transplantation* 2000; **70**: 157–9.
19 Krebs HA, Gascoyne T, Notton BM. Generation of extramitochondrial reducing power in gluconeogenesis. *Biochem J* 1967; **102**: 275–82.
20 Naito E, Ito M, Matsuura S *et al.* Type II citrullinemia (citrin deficiency) in a neonate with hypergalactosemia detected by mass screening. *J Inherit Metab Dis* 2002; **25**: 71–6.
21 Langer R, Glaser L. Interaction of nucleotides with liver uridine dinucleotide-glucose-4'-epimerase. *J Biol Chem* 1874; **249**: 1126–32.
22 Ishak KJ, Sharp HL. Developmental anomalies and liver disease in childhood. In: MacSween RNM, Burt AD, Portmann BC, Ishak KJ, Scheuer PJ, Anthony PP, eds. *Pathology of the Liver*, 4th edn. Edinburgh: Churchill Livingstone, 2003; 107–54.
23 Becroft DMO. Syndrome of encephalopathy and fatty degeneration of viscera in New Zealand children. *Br Med J* 1966; **2**: 135–40.
24 Pint HC, Baptista A, Camilo ME *et al.* Nonalcholic steatohepatitis. Clinicopathlogical comparison with alcholic hepatitis in ambulatory and hospitalized patients. *Dig Dis Sci* 1996; **41**: 172–9.

Molecular Genetics and Metabolism 100 (2010) 339–344

Contents lists available at ScienceDirect

Molecular Genetics and Metabolism

journal homepage: www.elsevier.com/locate/ymgme

A novel mutation (c.951C>T) in an exonic splicing enhancer results in exon 10 skipping in the human mitochondrial acetoacetyl-CoA thiolase gene

Toshiyuki Fukao [a,b,*], Reiko Horikawa [c], Yasuhiro Naiki [c], Toju Tanaka [d], Masaki Takayanagi [e], Seiji Yamaguchi [f], Naomi Kondo [a]

[a] Department of Pediatrics, Graduate School of Medicine, Gifu University, Gifu 501-1194, Japan
[b] Medical Information Sciences Division, United Graduate School of Drug Discovery and Medical Information Sciences, Gifu University, Gifu 501-1196, Japan
[c] Division of Endocrinology and Metabolism, National Center for Child Health and Development, Tokyo 157-8535, Japan
[d] Division of Clinical Genetics and Molecular Medicine, National Center for Child Health and Development, Tokyo 157-8535, Japan
[e] Chiba Children's Hospital, Chiba 266-0007, Japan
[f] Department of Pediatrics, Faculty of Medicine, Shimane University, Izumo, Shimane 693-8501, Japan

ARTICLE INFO

Article history:
Received 9 February 2010
Received in revised form 16 March 2010
Accepted 16 March 2010
Available online 19 March 2010

Keywords:
Aberrant splicing
Exonic mutation
Splice site selection
Mitochondrial acetoacetyl-CoA thiolase
Inborn error of metabolism
SF2/ASF

ABSTRACT

Mitochondrial acetoacetyl-CoA thiolase (T2) deficiency is an inherited disorder affecting isoleucine catabolism and ketone body metabolism. A Japanese female developed a severe ketoacidotic attack at the age of 7 months. Urinary organic acid analysis showed elevated excretion of 2-methyl-3-hydroxybutyrate but not tiglylglycine. She was diagnosed as having T2 deficiency by enzyme assay using fibroblasts. Mutation analysis revealed a compound heterozygote of c.556G>T(D186Y) and c.951C>T(D317D). Since c.951C>T does not cause amino acid change, we performed cDNA analysis and found that exon 10 skipping had occurred in the c.951C>T allele. A computer search using an ESE finder showed that an exonic splicing enhancer sequence, SF2/ASF, was located in CTGA^{951}CGC. We hypothesized that the exonic splicing enhancer is necessary for accurate splicing since the first nucleotide of exon 10 is C, which weakens the splice acceptor site of intron 9. We made a mini gene construct including exon 9-truncated intron 9-exon 10-truncated intron 10-exon 11 for a splicing experiment. We also made three mutant constructs which alter the SF2/ASF site (947C>T, 951C>T, 952G>A). An min-gene splicing experiment clearly showed that exon 10 skipping was induced in all three mutant constructs. Moreover, additional substitution of G for C at the first nucleotide of exon 10 resulted in normal splicing in these three mutants. These results confirmed that c.951C>T diminished the effect of the exonic splicing enhancer and caused exon 10 skipping.

Introduction

Mitochondrial acetoacetyl-CoA thiolase (T2[1]) (EC 2.3.1.9, gene symbol *ACAT1*) deficiency (OMIM 203750, 607809) is an autosomal recessive disorder, commonly known as β-ketothiolase deficiency. Since 1971 [1], more than 70 patients with it have been identified (including personal communications) [2]. This disorder affects the catabolism of isoleucine and the metabolism of ketone bodies, and is clinically characterized by intermittent ketoacidotic episodes with no clinical symptoms between episodes. T2-deficient patients usually have urinary excretion of 2-methyl-3-hydroxybutyrate, 2-methylacetoacetate and tiglylglycine, derived from intermediates in isoleucine catabolism. The severity of the clinical features varies from patient to patient but follow-up studies reveal that, in general, T2 deficiency has a favorable outcome [3].

The T2 gene (gene symbol: ACAT1) spans approximately 27 kb, contains 12 exons [4], and is located at 11q22.3–q23.1 [5]. Human T2 cDNA is about 1.5 kb long and encodes a precursor protein of 427 amino acids, including a 33-amino-acid leader polypeptide [6]. We have identified more than 70 gene mutations [7–25], 15% of which cause aberrant splicing. Most were located at the highly conserved ag at the splice acceptor site and gt at the splice donor site. We also identified some exonic mutations which cause aberrant splicing by activating cryptic splice sites within their exons [15,24].

We herein report a novel exonic mutation—c.951C>T (the 11th nucleotide in exon 10). It was first regarded to be a silent mutation, D317D, but was associated with exon 10 skipping in cDNA analysis. The c.951C nucleotide is located in a possible exonic splicing enhancer (ESE) sequence, SF2/ASF, and C>T substitution results in a deviation from its consensus sequence. We showed by a

* Corresponding author at: Department of Pediatrics, Graduate School of Medicine, Gifu University, 1-1 Yanagido, Gifu 501-1194, Japan. Fax: +81 58 230 6387.
E-mail address: toshi-gif@umin.net (T. Fukao).

[1] *Abbreviation used:* T2, mitochondrial acetoacetyl-CoA thiolase.

1096-7192/$ - see front matter © 2010 Elsevier Inc. All rights reserved.
doi:10.1016/j.ymgme.2010.03.012

minigene splicing experiment that the substitutions in this ESE caused exon 10 skipping.

Materials and methods

Case report

The patient (GK64), a female, was born to non-consanguineous Japanese parents. She was well until 7 months of age when she presented with a one-week history of coughing and appetite loss. She developed convulsions and was admitted to a hospital. Laboratory findings showed blood pH 6.769, bicarbonate 2.8 mmol/L, base excess −28.2 mmol/L, ammonia 213 μmol/L, and blood glucose 0.45 mmol/L. She was referred to the National Center for Child Health and Development on a mechanical ventilation support. Urinary organic acid analysis at the time of crisis showed huge amounts of acetoacetate and 3-hydroxybutyrate with dicarboxylic acids; 2-methyl-3-hydroxybutyrate and tiglylglycine were not evident at that time. She was successfully treated by intravenous glucose infusion. Later, she had an upper respiratory infection and her urinary ketone was 2+ at the age of 8 months. At that time, urinary organic acid analysis showed the presence of 2-methyl-3-hydroxybutyrate. However, tiglylglycine, another characteristic urinary organic acid in T2 deficiency, was not detected. Skin biopsy and a fibroblast culture were performed and finally she was diagnosed as having T2 deficiency by enzyme assay.

Cell culture, enzyme assay and immunoblot analysis

The fibroblasts were cultured in Eagle's minimum essential medium containing 10% fetal calf serum. Acetoacetyl-CoA thiolase activity was assayed, as described in [26]. Immunoblot analysis was done, as described in [27].

Mutation detection

Genomic DNA was purified from the fibroblasts with Sepa Gene kits (Sanko Junyaku, Tokyo, Japan). Mutation screening was performed at the genomic level by PCR and direct sequencing using a primer set for 12 fragments including an exon and its intron boundaries [13]. RNA was prepared from the fibroblasts using an ISOGEN kit (Nippon Gene, Tokyo, Japan). RT-PCR and sequencing after subcloning into a pGEM-T Easy vector (Promega, Madison, USA) were performed as described previously [7], except for the following point. A full-coding sequence of human T2 cDNA was amplified as a single fragment using a sense primer (5′-$^{-40}$AGTCTACGCCTGTGGAGCCGA^{-20}-3′) and an antisense primer (5′-^{1326}TTCTGGTCACATAGGGTT^{1309}-3′).

Transient expression analyses

Transient expression analysis of T2 cDNAs was done using a pCAGGS eukaryote expression vector [28], as described in [19]. After transfection, the cells were further cultured at 37 °C for 72 h, and then they were harvested and kept at −80 °C until use. The cells were freeze-thawed and sonicated in 50 mM sodium phosphate (pH 8.0), 0.1% Triton X-100. After centrifugation at 10,000*g* for 10 min, the supernatant was used in an enzyme assay for acetoacetyl-CoA thiolase activity and for immunoblot analysis.

Splicing experiment

A fragment (about 4 kb long) from the middle part of exon 9 to the middle part of exon 11 was amplified by Phusion DNA polymerase (New England BioLabs, Ipswich, USA) using control genomic DNA. The primers used in this amplification included the EcoR I linker sequence, as follows:

Ex 9 (EcoR I) primer (exon 9, sense) 5′-cagctgcgaatt^{842}CCAGTAC ACTGAATGATGGAGCAGCT^{873}-3′.

Ex 11 (EcoR I) primer (exon 11, antisense) 5′-cctccattggaatt^{1122}C ACTTTTTGGGGATCAATCT^{1103}-3′.

The amplified fragment, after digestion with EcoR I, was subcloned into an EcoR I site of the pCAGGS expression vector from which the Hind III and Pst I sites were deleted. The subcloned PCR fragment did not contain PCR errors, at least in the sequence of exon 9, the 3′ and 5′ splice sites of intron 9, exon 10, the 3′ and 5′ splice sites of intron 10, and exon 11. We deleted about a 0.5-kb Hind III-Pst I inner fragment in intron 9 and a 1.1-kb Hind III-Pst I inner fragment in intron 10 to reduce the minigene construct length. In order to make an mutant construct, in vitro mutagenesis was done on the wild-type fragment in the pUC118 vector, and then the mutant fragment was subcloned into the pCAGGS expression vector as a cassette of an about 870-bp Pst I-Hind III fragment including exon 10. We made three mutant constructs which altered the SF2/ASF site (c.947C>T, c.951C>T, and c.952G>A). Moreover, we also made three further mutant constructs with additional substitution of c.941G for C at the first nucleotide of exon 10.

Two μg of these expression vectors were transfected into 5×10^5 cells of SV40-transformed fibroblasts using Lipofectamine 2000. At 48 h after transfection, RNA was extracted from the cells. The first-strand cDNA was transcribed with a rabbit β-globin-specific antisense primer (β-glo2) (5′-^{461}AGCCACCACCTTCTGATA-3′) and then amplified with the Ex10 (EcoRI) primer on T2 exon 10, and another rabbit-specific antisense primer (β-glo3) (5′-^{443}GGCAGCCTGCACCTGAGGAGT-3′) to amplify the chimera cDNA of human T2 and rabbit β-globin.

Allele-specific RT-PCR

We performed allele-specific RT-PCR using mismatched primers:

c.556G allele (D186)-specific sense primer, 5′-^{530}TTTGATTGTA AAA GACGGGCTATCT**G**^{556}-3′.

c.556T allele (Y186)-specific sense primer, 5′-^{530}TTTGATTGTA AAA GACGGGCTATCT**T**^{556}-3′

The bold G or T represents the D186Y mutation site of c.556G>A. The underlined T indicates a mismatch introduced to the 4th nucleotide to assist allele-specific-RT-PCR.

Antisense primer 5′-^{1065}GGCTTCTTTACTTCCCACATTGCA^{1041}-3′.

cDNA with exon 10 gave a 535-bp fragment and cDNA with exon 10 skipping gave a 470-bp fragment.

Results and discussion

Enzyme assay and immunoblot analysis

Potassium-ion-activated acetoacetyl-CoA thiolase activity was absent in GK64's fibroblasts (−K^+ 3.8, +K^+ 3.9 nmol/min/mg of protein; Control fibroblasts −K^+ 4.7, +K^+ 7.8 nmol/min/mg of protein), confirming the diagnosis of T2 deficiency. Succinyl-CoA:3-ketoacid CoA transferase activity was 6.3 nmol/min/mg of protein (control fibroblasts 5.6 nmol/min/mg of protein). In immunoblot analysis, GK64's fibroblasts had a reduced but significant amount of T2 protein (Fig. 1). We then performed immunoblot analysis using two-fold serially diluted samples of two controls and GK64's fibroblasts from 30 to 3.75 μg. The relative amount of T2 protein in GK64 fibroblasts were estimated to be 25% of controls (data not shown).

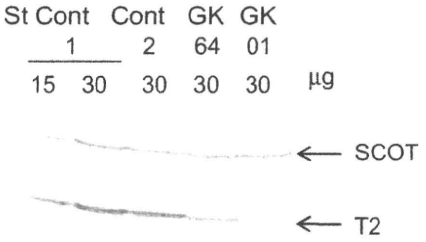

Fig. 1. Immunoblot analysis. The amount of fibroblast protein extract applied was indicated in each lane. The first antibody was a mixture of an anti-T2 antibody and an anti-SCOT antibody. The positions of the bands for T2 and SCOT are indicated by arrows. Cont 1 and Cont 2 were healthy controls and GK01 was a disease control being cross reactive material-negative.

Mutation screening at the genomic level and cDNA level

Routine genomic PCR and sequencing of exons 1–12 identified two nucleotide substitutions, c.556G>T(D186Y) in exon 6 and c.951C>T(D317D) in exon 10. Both c.556G>T and c.951C>T were novel nucleotide substitutions in the T2 gene. No further mutations were identified by genomic mutation screening. Since the latter substitution does not alter amino acid, we performed RT-PCR analysis. A full-coding region was amplified using a pair of primers on a 5′-noncoding region and a 3′-non-coding region, allowing one to show the segregation of these two substitutions. After subcloning, 8 clones had c.556G>T(D186Y) but not c.951C>T(D317D). Two clones had exon 10 skipping without c.556G>T(D186Y). The exon 10 skipping causes a frame shift and premature termination at c.1011TAA. We re-sequenced the genomic region around exon 10 (IVS8 − 88–IVS9 + 44) again, but only c.951C>T(D317D) was detected. We regarded c.951C>T(D317D), the 11th nucleotide of exon 10, as the cause of exon 10 skipping which was detected in GK64's cDNA. Since the splice acceptor site of intron 9 might be weak because of the first nucleotide of exon 10 being C, we hypothesized that ESE sequences would be necessary for accurate exon recognition of exon 10 and that c.951C>T might disrupt the ESE and result in exon 10 skipping.

Transient expression analysis of D186Y mutant cDNA

Transfection of wild-type T2 cDNA gave a high acetoacetyl-CoA thiolase activity in the presence of potassium ion. Transfection of D186Y mutant cDNA gave no significant thiolase activity compared with mock cDNA transfection (Fig. 2A) Immunoblot analysis showed that mutant D186Y protein was detected with 1/3-fold amount of wild-type protein (Fig. 2B). These results indicate that the D186Y mutant protein is a stable protein but retains no residual activity. Even when incubation was done at a lower temperature (30 °C) after transfection, no residual T2 activity was detected (data not shown). This result confirmed that the D186Y mutation is a causative mutation in one allele, and is consistent with the fact that GK64's fibroblasts had T2 protein with about a 1/4-fold amount of controls'.

Searches for ESE sequence

We searched the possible ESE sequences which can be affected by c.951C>T, using ESE finder 3.0 (http://rulai.cshl.edu/cgi-bin/tools/ESE3/esefinder.cgi?process=home) [30–31] and found that this mutated site, c.951C>T, was located in a possible SF2/ASF site, c.947CTGA951CGC (7th–13th nucleotides in exon 10). The substitution made a deviation from the consensus sequence of SF2/ASF, as shown in Fig. 3A.

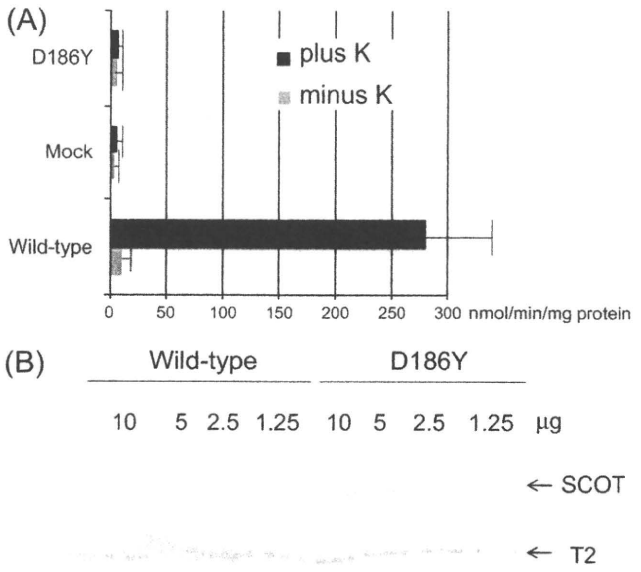

Fig. 2. Transient expression analysis of D186Y mutant cDNA. (A) Potassium-ion-activated acetoacetyl-CoA thiolase assay. Acetoacetyl-CoA thiolase activity in the supernatant of the cell extract was measured. The mean values of acetoacetyl-CoA thiolase activity in the absence and presence of the potassium ion are shown together with the standard deviation of three independent experiments. (B) Immunoblot analysis. The protein amounts applied are shown above the lanes. The first antibody was a mixture of an anti-T2 antibody and an anti-SCOT antibody.

Minigene splicing constructs

We previously successfully performed minigene splicing experiments using a pCAGGS expression vector [8,24,29]. Since our minigene construct produces human T2-rabbit β-globin fusion mRNA, we could amplify this specific mRNA by RT-PCR using a combination of a human T2 sense primer and a rabbit β-globin antisense primer. We made a minigene construct including exon 9-truncated intron 9-exon 10-truncated intron 10-exon 11 for a splicing experiment, as shown in Fig. 3B. We made the c.951C>T mutant constructs and two additional mutant constructs (c.947C>T or c.952G>A) which also altered the SF2/ASF site, as shown in Fig. 3A. We hypothesized that the ESE is necessary for accurate splicing since the first nucleotide of exon 10 is C, which weakens the splice acceptor site of intron 9. Hence, we made three constructs with an additional substitution of 941G for C at the first nucleotide of exon 10 to strengthen the splice acceptor site of intron 9.

Splicing experiment

We performed a minigene splicing experiment. As shown in Fig. 3C, exon 10 skipping was induced in all three mutant constructs. Normally spliced transcripts with the inclusion of exon 10 were also produced in these mutant transcripts. The ratio of signal intensity of transcripts with exon 10 skipping to that of normally spliced transcripts in three independent experiments was highest in c.951C>T, followed by c.952G>A among these three mutants.

Moreover, additional substitution of G for C at the first nucleotide of exon 10 resulted in normal splicing in these three mutants. Hence, the ESE (SF2/ASF) was only necessary in the case of C at the first nucleotide of exon 10 in the experiment. This clearly showed that c.941C, the first nucleotide of exon 10, makes the recognition

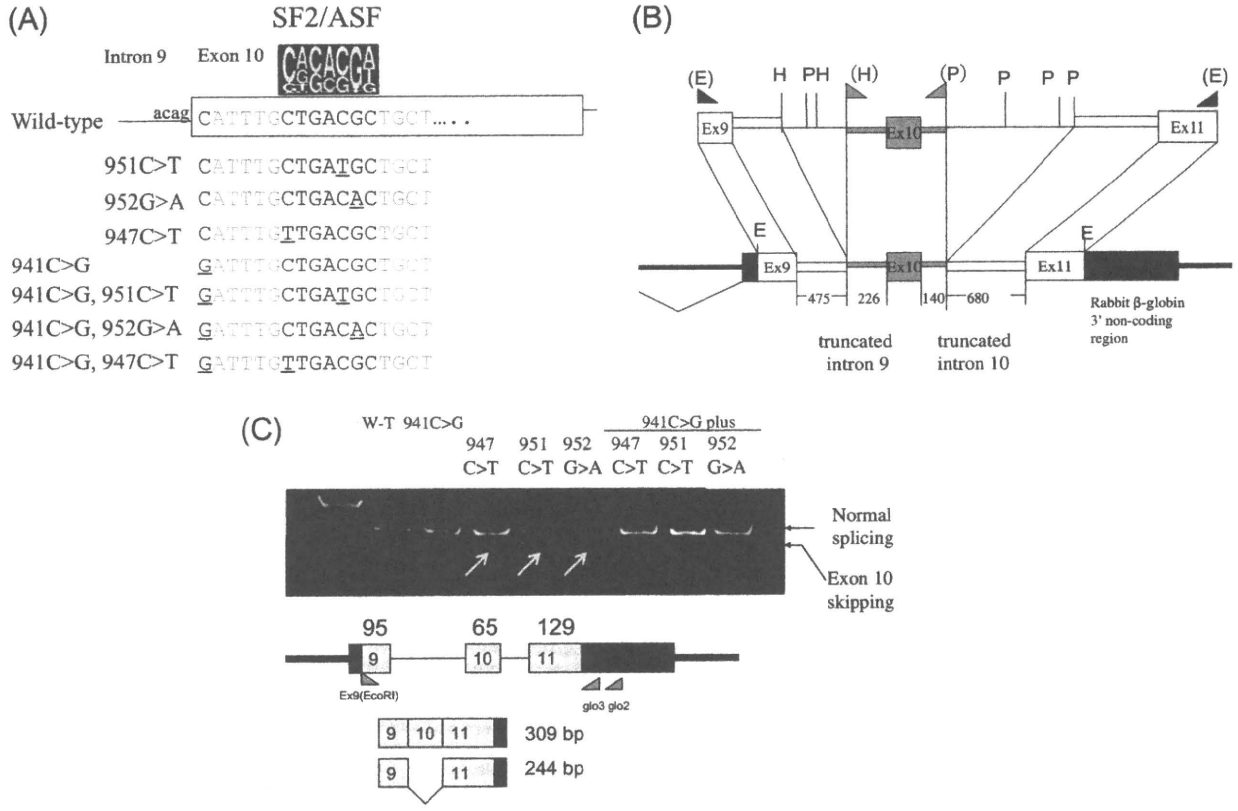

Fig. 3. Minigene splicing experiment. (A) Minigene splicing constructs. Sequence differences among 8 minigene splicing constructs. Mutations introduced are underlined. (B) Schematic presentation of minigene splicing construct. The minigene construct has a T2 gene fragment from c.842 of exon 9 and intron 9 (from +1 to a Hind III site, 475-bp open box) and intron 10 (from a Pst I site to −1, 680-bp open box) and exon 11 (to c. 1122). In the cases of mutant constructs, the region around exon 10, highlighted in gray, was replaced as a cassette. Thick lines and black boxes indicate pCAGGS vector sequences. (C) Detection of chimeric cDNAs derived from transfected minigenes. First-strand cDNA was reverse-transcribed using the glo2 primer. cDNA amplification was done using Ex9(EcoRI) and glo3 primers. Normal splicing and aberrant splicing produced 309-bp and 244-bp PCR fragments, respectively. The PCR fragments were electrophoresed on 5% polyacrylamide gel. Fragments with exon 10 skipping are shown by arrows.

of exon 10 or the splice acceptor site of intron 9 and requires an ESE for the accurate splicing of exon 10. These results confirmed that c.951C>T diminished the effect of the ESE and caused exon 10 skipping.

Effects of c.951C>T mutation on splicing

In the minigene splicing, normally spliced transcripts were detected in the construct with c.951C>T. This may mean that not only exon-10-skipped transcripts but also normally spliced transcripts can be produced in the c.951C>T mutant allele. However, when we analyzed 10 clones of full-length cDNA, 8 clones were from the allele with c.556G>T(D186Y). Two clones had exon 10 skipping but no cDNA clones with c.951C>T were found. In direct sequencing of full-length cDNA fragments, we found a possible faint signal for c.951T in the major signal for c.951C (Fig. 4B). Hence, the presence of normally spliced transcripts from c.951C>T was further confirmed by allele-specific RT-PCR. As shown in Fig. 4A, both c.556T(Y186) allele- and c.556G(D186) allele-specific RT-PCR gave a fragment with the expected size in the case of GK64, and only the latter gave a fragment in the case of a control. In direct sequencing of GK64's fragment of the c.556G(D186) allele, c.951 was T (normally spliced transcripts in the c.951C>T mutant allele) (Fig. 4B). An additional faint fragment with exon 10 skipping was also seen in GK64's c.556G(D186) allele-specific PCR. Exon 10 skipping causes frame shift and should result in nonsense-mediated mRNA decay; hence, the amount of cDNA with exon 10 skipping in the D186 allele was smaller than that of normally spliced cDNA. Based

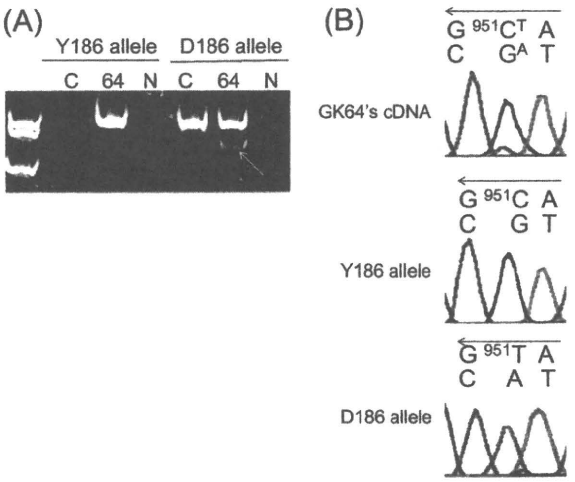

Fig. 4. Allele-specific cDNA amplification. (A) Allele-specific PCR fragments were electrophoresed on 5% polyacrylamide gel. C, control cDNA; 64, GK64's cDNA; N, negative control. An arrow indicates cDNA with exon 10 skipping. (B) Direct sequencing of the antisense strand at the c.951c>T (D186Y) site. Y186 allele, Y186 allele-specific PCR fragment; D186 allele, D186 allele-specific PCR fragment.

on cDNA analysis, a small amount of normally spliced mRNA with c.951C>T(D317D) was also produced and hence GK64 retained some residual T2 activity from this mutant allele. This finding is in accord with GK64's urinary organic acid profiles. We previously

showed that urinary organic acid analysis shows no elevated tiglylglycine and relatively small amount of 2-methyl-3-hydroxybutyrate even during ketoacidotic crisis and subtle elevation of 2-methyl-3-hydroxybutyrate under stable conditions in patients with mutations which retain some residual T2 activity [3,18,19].

The importance of the exonic splicing enhancer

The accurate removal of introns from pre-mRNA is essential for correct gene expression. However, the information contained in splice sites, including the splice donor site, branch site and splice acceptor site, is insufficient for a precise definition of exons [32–35]. Recently, it was established that exon sequence has elements which contribute to exonic recognition. Additional regulatory elements exist in the form of ESEs [32,33]. Exonic variants may inactivate an ESE, resulting in insufficient exon inclusion.

ESEs are known to play a particularly important role in exons with weak splice sites. Although the splice acceptor site of intron 10 has a relatively high Shapiro and Senapathy score [35] of 90.5, the site deviates from the consensus sequence at position +1, by the replacement of the G nucleotide with C. In computèr analysis using ESE finder, the mutation c.951C>T was located on an ESE, the SF2/ASF site. SF2/ASF is a prototypical serine- and arginine-rich protein (SR family) with important roles in splicing and other aspects of mRNA metabolism. One classical function of SR proteins bound to exonic sequences is to stimulate recognition of the flanking splice sites [36]. Using the minigene approach, we have demonstrated that not only the c.951C>T substitution but also c.947C>T and c.952G>A, all of which affected the SF2/ASF site, resulted in insufficient exon 10 inclusion. This phenomenon was completely corrected by a substitution of G for C at the first nucleotide of exon 10. We therefore suggest that the weak splice acceptor site of intron 10 is normally compensated for by an ESE (SF2/ASF).

There are several precedent reports on ESE mutations in other genes [37–39]. For example, two synonymous mutations in exon 5 identified in pyruvate dehydrogenase-deficient patients (the c.483C>T and c.498C>T variants) disrupt a putative ESE, the SRp55 binding site [37]. These synonymous mutations result in the incomplete inclusion of PDHA1 exon 5 in the minigene splicing experiment and this effect is corrected following the restoration of a perfect consensus sequence for the 5′ splice site by site-directed mutagenesis. The mutation in the SRp55 binding site is affected in the case of the weak 5′ splice site selection in this case and the mutation in SF2/ASF site was affected in the case of the weak 3′ splice site selection in our case. c.1918C>G (pR640G) in exon 14 in the APC gene, which was found in a familial adenomatous polyposis (FAP) patient, was revealed to be sufficient to cause exon 14 skipping [38]. Minigene splicing experiments showed a mechanism involving disruption of an ASF/SF2 element. Systemic analysis of 24 mutations in PAH exon 9 showed that three of them affected ESE motifs and resulted in exon 9 skipping [39]. These facts indicate that we should consider that any mutations in an exon may affect splicing of the exon.

Importance of cDNA analysis

If mutation analysis were done only at the genomic level, this c.951C>T(D317D) mutation would be regarded as a silent mutation. However, the main character of this mutation was an ESE mutation which causes exon 10 skipping. Any nucleotide substitutions have the possibility to affect splicing efficiency. This indicates the importance of cDNA analysis to understand the character of mutations properly.

Acknowledgments

We thank N. Sakaguchi and K. Murase for technical assistance.

This study was supported in part by a Grant-in-Aid for Scientific Research from the Ministry of Education, Science, Sports and Culture of Japan and by Health and Labor Science Research Grants for Research on Intractable Diseases and For Research on Children and Families from The Ministry of Health, Labor and Welfare of Japan.

References

[1] R.S. Daum, P. Lamm, O.A. Mamer, C.R. Scriver, A "new" disorder of isoleucine catabolism, Lancet 2 (1971) 1289–1290.
[2] G.A. Mitchell, T. Fukao, Chapter 102, Inborn errors of ketone body metabolism, in: C.R. Scriver, A.L. Beaudet, W.S. Sly, D. Valle (Eds.), Metabolic and Molecular Bases of Inherited Disease, eighth ed., McGraw-Hill, Inc., New York, 2001, pp. 2327–2356.
[3] T. Fukao, C.R. Scriver, N. Kondo, T2 Collaborative Working Group, The clinical phenotype and outcome of mitochondrial acetoacetyl-CoA thiolase deficiency (b-ketothiolase deficiency) in 26 enzymatically proved and mutation defined patients, Mol. Genet. Metab. 72 (2001) 109–114.
[4] M. Kano, T. Fukao, S. Yamaguchi, T. Orii, T. Osumi, T. Hashimoto, Structure and expression of the human mitochondrial acetoacetyl-CoA thiolase-encoding gene, Gene 109 (1991) 285–290.
[5] M. Masuno, M. Kano, T. Fukao, S. Yamaguchi, T. Osumi, T. Hashimoto, E. Takahashi, T. Hori, T. Orii, Chromosome mapping of the human mitochondrial acetoacetyl-coenzyme A thiolase gene to 11q22.3–q23.1 by fluorescence in situ hybridization, Cytogenet. Cell Genet. 60 (1992) 121–122.
[6] T. Fukao, S. Yamaguchi, M. Kano, T. Orii, Y. Fujiki, T. Osumi, T. Hashimoto, Molecular cloning and sequence of the complementary DNA encoding human mitochondrial acetoacetyl-coenzyme A thiolase and study of the variant enzymes in cultured fibroblasts from patients with 3-ketothiolase deficiency, J. Clin. Invest. 86 (1990) 2086–2092.
[7] T. Fukao, S. Yamaguchi, T. Orii, R.B.H. Schutgens, T. Osumi, T. Hashimoto, Identification of three mutant alleles of the gene for mitochondrial acetoacetyl-CoA thiolase: a complete analysis of two generations of a family with 3-ketothiolase deficiency, J. Clin. Invest. 89 (1992) 474–479.
[8] T. Fukao, S. Yamaguchi, A. Wakazono, T. Orii, G. Hoganson, T. Hashimoto, Identification of a novel exonic mutation at −13 from 5′ splice site causing exon skipping in a girl with mitochondrial acetoacetyl-coenzyme A thiolase deficiency, J. Clin. Invest. 93 (1994) 1035–1041.
[9] T. Fukao, S. Yamaguchi, T. Orii, T. Hashimoto, Molecular basis of beta-ketothiolase deficiency: mutations and polymorphisms in the human mitochondrial acetoacetyl-coenzyme A thiolase gene, Hum. Mutat. 5 (1995) 113–120.
[10] T. Fukao, X.Q. Song, S. Yamaguchi, T. Orii, R.J.A. Wanders, B.T. Poll-The, T. Hashimoto, Mitochondrial acetoacetyl-coenzyme A thiolase gene: a novel 68-bp deletion involving 3′ splice site of intron 7, causing exon 8 skipping in a Caucasian patient with beta-ketothiolase deficiency, Hum. Mutat. 5 (1995) 94–96.
[11] A. Wakazono, T. Fukao, S. Yamaguchi, Y. Hori, T. Orii, M. Lambert, G.A. Mitchell, G.W. Lee, T. Hashimoto, Molecular and biochemical, and clinical characterization of mitochondrial acetoacetyl-coenzyme A thiolase deficiency in two further patients, Hum. Mutat. 5 (1995) 34–42.
[12] T. Fukao, X.Q. Song, S. Yamaguchi, N. Kondo, T. Orii, J.M. Matthieu, C. Bachmann, T. Orii, Identification of three novel frameshift mutations (83delAT, 754indCT, and 435+1G to A) of mitochondrial acetoacetyl-coenzyme A thiolase gene in two Swiss patients with CRM-negative beta-ketothiolase deficiency, Hum. Mutat. 9 (1997) 277–279.
[13] T. Fukao, H. Nakamura, X.Q. Song, K. Nakamura, K.E. Orii, Y. Kohno, M. Kano, S. Yamaguchi, T. Hashimoto, T. Orii, N. Kondo, Characterization of N93S, I312T, and A333P missense mutations in two Japanese families with mitochondrial acetoacetyl-CoA thiolase deficiency, Hum. Mutat. 2 (1998) 245–254.
[14] A.C. Sewell, J. Herwig, I. Wiegratz, W. Lehnert, H. Niederhoff, X.Q. Song, N. Kondo, T. Fukao, Mitochondrial acetoacetyl-CoA thiolase (beta-keto-thiolase) deficiency and pregnancy, J. Inherit. Metab. Dis. 21 (1998) 441–442.
[15] K. Nakamura, T. Fukao, C. Perez-Cerda, C. Luque, X.Q. Song, Y. Naiki, Y. Kohno, M. Ugarte, N. Kondo, A novel single-base substitution (380C>T) that activates a 5-base downstream cryptic splice-acceptor site within exon 5 in almost all transcripts in the human mitochondrial acetoacetyl-CoA thiolase gene, Mol. Genet. Metab. 72 (2001) 115–121.
[16] T. Fukao, H. Nakamura, K. Nakamura, C. Perez-Cerda, A. Baldellou, C.R. Barrionuevo, F.G. Castello, Y. Kohno, M. Ugarte, N. Kondo, Characterization of 6 mutations in 5 Spanish patients with mitochondrial acetoacetyl-CoA thiolase deficiency: effects of amino acid substitutions on tertiary structure, Mol. Genet. Metab. 75 (2002) 235–243.
[17] T. Fukao, N. Matsuo, G.X. Zhang, R. Urasawa, T. Kubo, Y. Kohno, N. Kondo, Single base substitutions at the initiator codon in the mitochondrial acetoacetyl-CoA thiolase (ACAT1/T2) gene result in production of varying amounts of wild-type T2 polypeptide, Hum. Mutat. 21 (2003) 587–592.

[18] T. Fukao, G-X Zhang, N. Sakura, T. Kubo, H. Yamaga, H. Hazama, Y. Kohno, N. Matsuo, M. Kondo, S. Yamaguchi, Y. Shigematsu, N. Kondo, The mitochondrial acetoacetyl-CoA thiolase deficiency in Japanese patients: urinary organic acid and blood acylcarnitine profiles under stable conditions have subtle abnormalities in T2-deficient patients with some residual T2 activity, J. Inherit. Metab. Dis. 26 (2003) 423–431.
[19] G.X. Zhang, T. Fukao, M.O. Rolland, M.T. Zabot, G. Renom, E. Touma, M. Kondo, N. Matsuo, N. Kondo, The mitochondrial acetoacetyl-CoA thiolase (T2) deficiency: T2-deficient patients with mild mutation(s) were previously misinterpreted as normal by the coupled assay with tiglyl-CoA, Pediatr. Res. 56 (2004) 60–64.
[20] L. Mrazova, T. Fukao, K. Halovd, E. Gregova, V. Kohut, D. Pribyl, P. Chrastina, N. Kondo, E. Pospisilova, Two novel mutations in mitochondrial acetoacetyl-CoA thiolase deficiency, J. Inherit. Metab. Dis. 28 (2005) 235–236.
[21] G.X. Zhang, T. Fukao, S. Sakurai, K. Yamada, K.M. Gibson, N. Kondo, Identification of Alu-mediated, large deletion-spanning exons 2–4 in a patient with mitochondrial acetoacetyl-CoA thiolase deficiency, Mol. Genet. Metab. 89 (2006) 222–226.
[22] S. Sakurai, T. Fukao, A.M. Haapalainen, G. Zhang, S. Yamada, F. Lilliu, S. Yano, P. Robinson, M.K. Gibson, R.J.A. Wanders, G.A. Mitchell, R.K. Wierenga, N. Kondo, Kinetic and expression analyses of seven novel mutations in mitochondrial acetoacetyl-CoA thiolase (T2): identification of a Km mutant and an analysis of the mutational sites in the structure, Mol. Genet. Metab. 90 (2007) 370–378.
[23] T. Fukao, G. Zhang, M-O. Rolland, M-T. Zabot, N. Guffon, Y. Aoki, N. Kondo, Identification of an Alu-mediated tandem duplication of exons 8 and 9 in a patient with mitochondrial acetoacetyl-CoA thiolase (T2) deficiency, Mol. Genet. Metab. 92 (2007) 375–378.
[24] T. Fukao, A. Boneh, Y. Aoki, N. Kondo, A novel single-base substitution (c.1124A>G) that activates a 5-base upstream cryptic splice donor site within exon 11 in the human mitochondrial acetoacetyl-CoA thiolase gene, Mol. Genet. Metab. 94 (2008) 417–421.
[25] S. Thümmler, D. Dupont, C. Acquaviva, T. Fukao, D. de Ricaud, Different clinical presentation in siblings with mitochondrial acetoacetyl-CoA thiolase deficiency and identification of two novel mutations, Tohoku J. Exp. Med. 220 (2010) 27–31.
[26] T. Fukao, X.Q. Song, S. Yamaguchi, T. Hashimoto, T. Orii, N. Kondo, Immunotitration analysis of cytocolic acetoacetyl-coenzyme A thiolase activity in human fibroblasts, Pediatr. Res. 39 (1996) 1055–1058.
[27] T. Fukao, X.Q. Song, G.A. Mitchell, S. Yamaguchi, K. Sukegawa, T. Orii, N. Kondo, Enzymes of ketone body utilization in human tissues: protein and mRNA levels of succinyl-CoA: 3-ketoacid CoA transferase and mitochondrial and cytosolic acetoacetyl-CoA thiolases, Pediatr. Res. 42 (1997) 498–502.
[28] H. Niwa, K. Yamamura, J. Miyazaki, Efficient selection for high-expression transfectants with a novel eukaryotic vector, Gene 108 (1991) 192–200.
[29] H. Watanabe, K.E. Orii, T. Fukao, X-Q. Song, T. Aoyama, L. IJlst, J. Ruiter, R.J.A. Wanders, N. Kondo, Molecular basis of very long chain acyl-CoA dehydrogenase deficiency in three Israeli patients: identification of a complex mutant allele with P65L and K247Q mutations, the former being an exonic mutation causing exon 3 skipping, Hum. Mutat. 15 (2000) 430–438.
[30] P.J. Smith, C. Zhang, J. Wang, S.L. Chew, M.Q. Zhang, A.R. Krainer, An increased specificity score matrix for the prediction of SF2/ASF-specific exonic splicing enhancers, Hum. Mol. Genet. 15 (2006) 2490–2508.
[31] L. Cartegni, J. Wang, Z. Zhu, M.Q. Zhang, A.R. Krainer, ESEfinder: a web resource to identify exonic splicing enhancers, Nucleic Acid Res. 31 (2003) 3568–3571.
[32] A.C. Goldstrohm, A.L. Greenleaf, M.A. Garcia-Blanco, Co-transcriptional splicing of pre-messenger RNAs: considerations for the mechanism of alternative splicing, Gene 277 (2001) 31–47.
[33] T.A. Cooper, W. Mattox, The regulation of splice-site selection, and its role in human disease, Am. J. Hum. Genet. 61 (1997) 259–266.
[34] B.L. Robbertson, G.J. Cote, S.M. Berget, Exon definition may facilitate splice site selection in RNAs with multiple exons, Mol. Cell. Biol. 10 (1990) 84–94.
[35] M.B. Shapiro, P. Senapathy, RNA splice junctions of different classes of eukaryotes: sequence statistics and functional implications in gene expression, Nucleic Acids Res. 15 (1987) 7155–7174.
[36] S. Lin, X.D. Fu, SR proteins and related factors in alternative splicing, Adv. Exp. Med. Biol. 623 (2007) 107–122.
[37] A. Boichard, L. Venet, T. Naas, A. Boutron, L. Chevret, H.O. de Baulny, P. De Lonlay, A. Legrand, P. Nordman, M. Brivet, Two silent substitutions in the PDHA1 gene cause exon 5 skipping by disruption of a putative exonic splicing enhancer, Mol. Genet. Metab. 93 (2008) 323–330.
[38] V. Gonçalves, P. Theisen, O. Antunes, A. Medeira, J.S. Ramos, P. Jordan, G. Isidro, A missense mutation in the APC tumor suppressor gene disrupts an ASF/SF2 splicing enhancer motif and causes pathogenic skipping of exon 14, Mutat. Res. 662 (2009) 33–36.
[39] P.Y. Ho, M.Z. Huang, V.T. Fwu, S.C. Lin, K.J. Hsiao, T.S. Su, Simultaneous assessment of the effects of exonic mutations on RNA splicing and protein functions, Biochem. Biophys. Res. Commun. 373 (2008) 515–520.